PCCP

Accepted Manuscript

ROYAL SOCIETY
OF CHEMISTRY

www.rsc.org/pccp

Molecular Dynamics of different Polymer Blends Containing Poly(2,6-dimethyl-1,4-phenylene ether)

Huan Wang[a,b], Baoqing Shentu*[b] and Roland Faller*[a]

[a] *Department of Chemical Engineering & Materials Science, University of California Davis, One Shields Ave, Davis, California 95616, United States*

[b]*State Key Lab of Chemical Engineering, Department of Chemical and Biological Engineering, Zhejiang University, Hangzhou 310027, China*

**Corresponding authors. Email: rfaller@ucdavis.edu; shentu@zju.edu.cn.*

Abstract:

Detailed atomistic molecular dynamics simulations were performed to investigate the behavior of two different binary blends, a miscible system poly(2,6-dimethyl-1,4-phenylene ether)/polystyrene (PPE/PS) and a immiscible system poly(2,6-dimethyl-1,4-phenylene ether)/poly(methyl methacrylate) (PPE/PMMA). We compared these two blends to study how PPE behaves when blended with different polymers. In both cases, the structure and phase behavior of polymer melts were studied by means of radial distribution functions (RDFs). Radii of gyration illustrate the static properties. Packing features of the benzene rings were observed in PPE and PS, both PS and PPE were well dispersed over the whole time scale of simulation. Furthermore, there was a tendency for aggregation of PMMA chains in PPE/PMMA system. The mean squared displacements of monomers and whole chains describe the mobility of polymers in various systems.

Keywords: Molecular dynamics simulation, poly(2,6-dimethyl-1,4-phenylene ether), polystyrene, poly(methyl methacrylate), miscibility

1. Introduction

Poly(2,6-dimethyl-1,4-phenylene ether) (PPE) also known as poly(2,6-dimethyl-1,4-phenylene oxide) (PPO) is a widely used engineering thermoplastic and has been applied in various fields due to its excellent electrical, chemical and mechanical properties.[1,2] However, the high glass transition temperature (T_g=210 °C), high melt viscosity and low oxidative stability of PPE make it difficult to process. Correspondingly, it is hardly used in its pure form and PPE is often blended with other polymers, such as polystyrene (PS) or poly(methyl methacrylate) (PMMA) to decrease the glass transition temperature.

The miscibility and phase behavior of different PPE blends have been widely studied by various experimental techniques.[2-10] For example, since PPE and PS are miscible over the complete composition range, a common commercial usage of PPE is as a PPE/PS blend, which became the most popular form of PPE blend.[2] In addition, the structural properties of PS melts with different molecular weights at various temperatures have been studied to some extent via both simulations and experiments.[11-14] PMMA is also an extensively studied polymer with a wide variety of applications due to its high transparency in visible light.[15] PPE is miscible with PMMA only for small molecular weights, and phase separates with increasing molecular weight.

Molecular dynamics has been widely used to investigate polymer blends [16-23]. It is well known that the components in miscible polymer blends have their own distinct segmental dynamics although they are in close contact with each other, and these components are biased to the dynamics of their pure forms. Furthermore, the Lodge-Mcleish model [24] has been employed to reveal the fact that the phenomena mentioned above is mainly caused by the enhanced local concentration as a result of chain connection. Similarly, immiscible polymer blends melt also possesses different local dynamics and a self concentration effect can be observed.[18] However, there are several open questions in how one polymer acts in various blend systems and what influences the phase behavior of a polymer in blends with different polymers although the effects of blending PPE with other polymers are well known on the large scale. In the present paper, we report the results of molecular dynamics (MD) simulations for two different linear polymer melt blends, PPE/PS and PPE/PMMA. We describe and compare the different behaviors of the three polymers in these two systems, as well as the mobility of polymer chains and monomers

2. Simulation Methods

Table 1 Number of chains in different polymer systems

DP	PPE	PMMA	PS	PPE/PMMA		PPE/PS	
				PPE	PMMA	PPE	PS
2	-	-	-	64	64	-	-
5	36	36	-	27	27	-	-
10	36	36	36	27	27	27	27
20	36	36	36	27	27	27	27
30	36	36	36	27	27	27	27

All atomistic, i.e. including all heavy atoms, MD simulations were performed using the LAMMPS code [25] and analysis was performed partially using VMD. [26] The polymer consistent force field (PCFF) [27-37] was used with a cutoff of 10 Å.

The boxes in all simulations were cubic with periodic boundary condition in all directions. For all systems, we first put one chain for each polymer in a cubic box, after minimizing the energy we replicated the box 26 times, so there were 27 chains for each polymer in the new box in total. Then all simulations were run in the *NPT* ensemble for 100 ns to equilibrate using a Nose-Hoover thermostat and barostat [25] with a timestep of 1 fs, the temperature and pressure damping parameters were set as 100 fs and 1000 fs, respectively. The temperature of all simulations was maintained at 480K which is slightly above the highest glass transition temperature of all mixtures to keep the blends in their melt state (glass transition temperature T_g=457K for PPE with degree of polymerization (DP)=30, T_g increases with the increasing of molecular weight, and T_g of PPE is the highest of the three polymers [38-41]). All pressures were controlled at p=1 atmosphere and the timestep was 1 fs. All polymer blends were 50:50 (by mol) mixed and all PS and PMMA chains were isotactic. The polymerization degree of each polymer chain (all systems are monodisperse) and the number of chains for the various systems are listed in Table 1. The curves of density versus simulation time of the mixtures were used to monitor the equilibration of all systems (cf. supplementary data). The density of two blends at 480 K in the melt state were measured to be 0.98 g/cm^{3}for PPE/PS and 1.06 g/cm^3 for PPE/PMMA, respectively using a Dilatometer DIL402C produced by Netzsch, Germany, in experiment. According to Figure S1 and S2, the equilibrated densities of all the PPE/PS blends are between 0.94 and 1.00 g/cm^3, while the equilibrated densities of PPE/PMMA blends range from 0.98 to 1.04 g/cm^3. The densities calculated in our simulations are reasonable for the polymers synthesized. Polymers in experiment possess much larger molecular weights and polydispersities than in the simulations.

Radii of gyration, were calculated every 20000 steps over 10000000 steps, and arithmetic average values were calculated. Mean squared displacements were calculated with a running time average (Nevery= 20, Nrepeat=100 and Nfreq=20000).

3. Results and discussion

3.1 Radial distribution functions

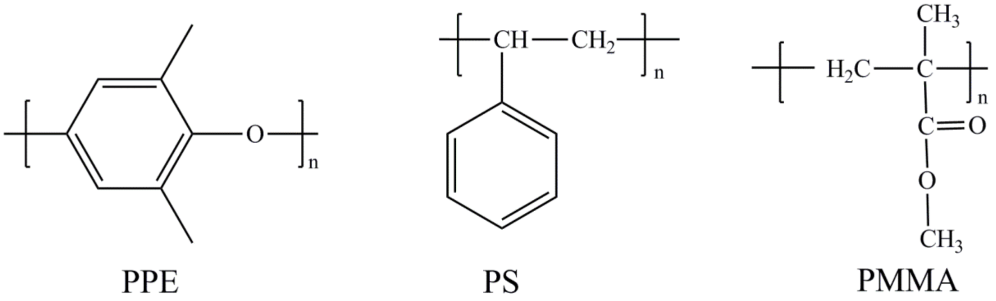

Scheme 1 Chemical structures of PPE, PMMA and PS

All polymers we model are linear and their structures are presented in Scheme 1. The backbone of PPE is mainly composed of benzene rings and only the C-O bonds have some flexibility, which makes the chains of PPE rather rigid. On the contrary, in PMMA the chain is quite flexible due to its C-C single-bond backbone, leading usually to a random-coil conformation. For PS the C-C bonds along the backbone make it flexible, but the benzene rings on the side chain add some hindrance, which makes PS neither as flexible as PMMA nor as rigid as PPE.

Radial distribution functions (RDF) are illustrative in characterizing the local structure. Figure 1 shows the RDFs of O in PPE for different chain lengths. The curves representing different chain lengths differ slightly due to the correlation hole effect (occurs because of a decreased interpenetration of chains) except for DP=2 where due to limited neighbors along the chain the last peak is missing. The peaks at about 4.8 Å are ascribed to the O in different chains and the peaks at about 9.5 Å correspond to the O belonging to the same chain. As the PPE dimer is the most rigid molecule almost no peak appears at 9.5 Å, and as the chains become more flexible with increasing chain length, some other small peaks appear when DP=20 and 30. RDFs of the carbonyl C in PMMA with various DPs are shown in Figure 2. Similar to PPE, curves representing polymers with different molecular weights do not change much. However, PMMA chains are more flexible than PPE chains, so only the change of peak sizes can be observed.

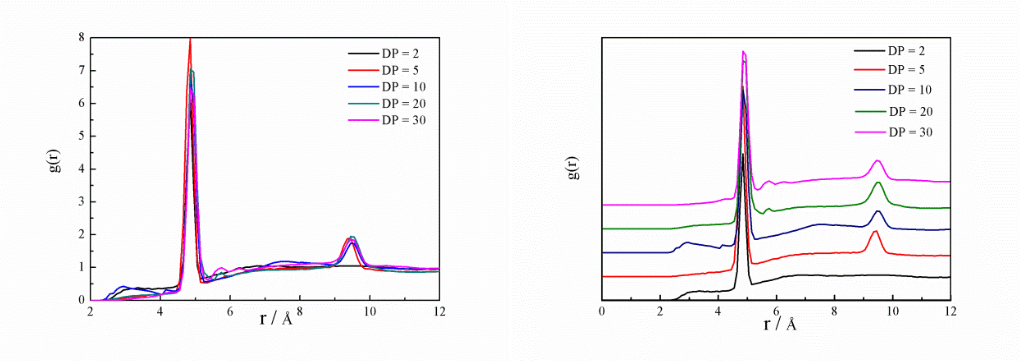

Figure 1 Radial distribution functions of O in PPE blended with PMMA

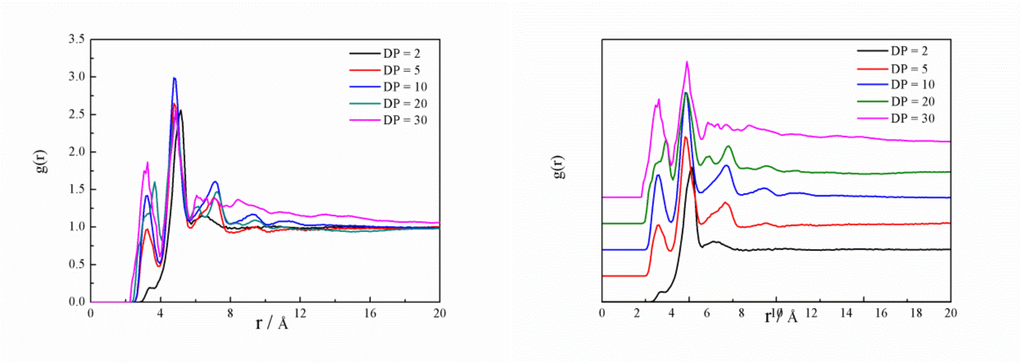

Figure 2 Radial distribution functions of carbonyl C in PMMA blended with PPE

Figure 3 shows the RDFs of O in PPE with the carbonyl C in PMMA. A peak at about 8 Å could be observed clearly for DP=2 and 5, respectively, and this peak becomes smaller when molecular weight increases. The peak can hardly be seen for DP=20 and almost disappears for DP=30, which indicates that phase separation sets in at DP=20. Furthermore, the small peaks between 2-5 Å become sharper for DP=20 and 30, this might be caused by the formation of a phase interface. When the molecular weight is small, chains of PPE and PMMA can distribute relatively evenly and the peak at 8 Å is obvious. When the molecular weight increases, the tendency to form a heterogeneous system becomes stronger, so the peak shrinks, and the small peaks between 2-5 Å turn sharper, indicating that only a small amount of atoms on the phase interface of each polymer are close to each other, and most atoms in different polymers tend to push each other away. A similar observation was reported by Jamieson et al where PPE was immiscible with PMMA and a compatibilizer was needed to emulsify [43].

The RDFs of the benzene C atoms in PPE with PS are shown in Figure 4. In contrast to PPE/PMMA, we see clearly that the three curves for different DP almost coincide with each other, suggesting that no phase separation happens in PPE/PS until DP=30, which is in good agreement with the experimental fact that a complete miscibility can be obtained below a critical molecular weight M_w=100000 [42]. There is also much local contact between chemically different chains. The peaks at about 1.3 Å indicate the packing of benzene rings between PPE and PS. Monomers of different chains approach each other typically with their benzene rings as contact. This might be a key factor that makes PPE and PS miscible over the complete composition range.

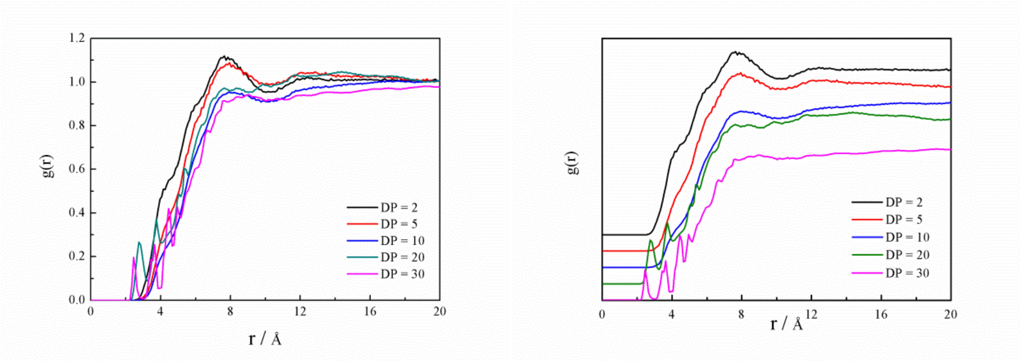

Figure 3 Radial distribution functions of O in PPE and carbonyl C in PMMA in PPE/PMMA

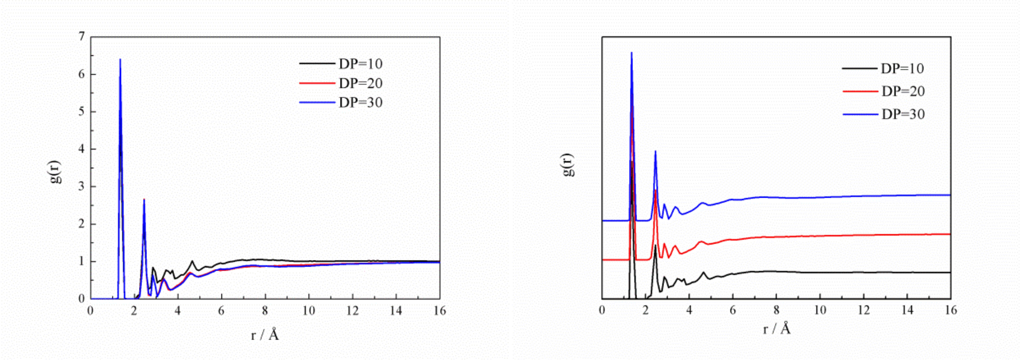

Figure 4 Radial distribution functions of benzene C in PPE/PS

RDFs cannot fully describe the packing structure of benzene rings in different polymer chains, thus the orientation correlation functions (OCF) of benzene rings are shown in Figure 5. The OCFs were calculated according to $P(r) = < \vec{u}_i \bullet \vec{u}_j >$ where, $\vec{u}_i$ and $\vec{u}_j$ represent the unit vector perpendicular to the plane of benzene rings in different chains, and the distance r is measured between the centers of mass of the benzene rings. The dihedral angle of two benzene rings is measured by the absolute value of P(r), thus whether the value of P(r) positive or negative does not affect the value of dihedral angle. When the absolute value of P(r) is close to 1, two benzene rings are almost parallel.

As shown in Figure 5, the OCFs of PPE/PS systems with different DPs are similar, and there are several strong peaks between 2 and 3 Å, indicating that benzene rings from different chains are almost parallel at close approach, and they are oriented randomly at larger distance. This shows that the packing dominates the behavior of the benzene rings at close distance, and this is important for understanding the miscibility of PPE/PS.

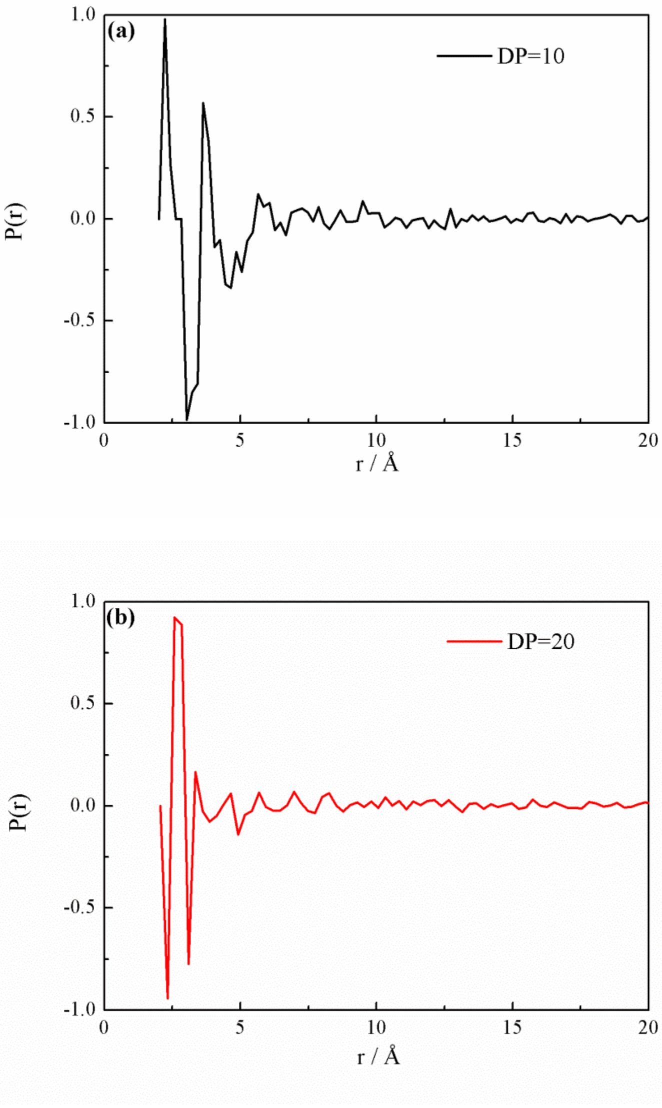

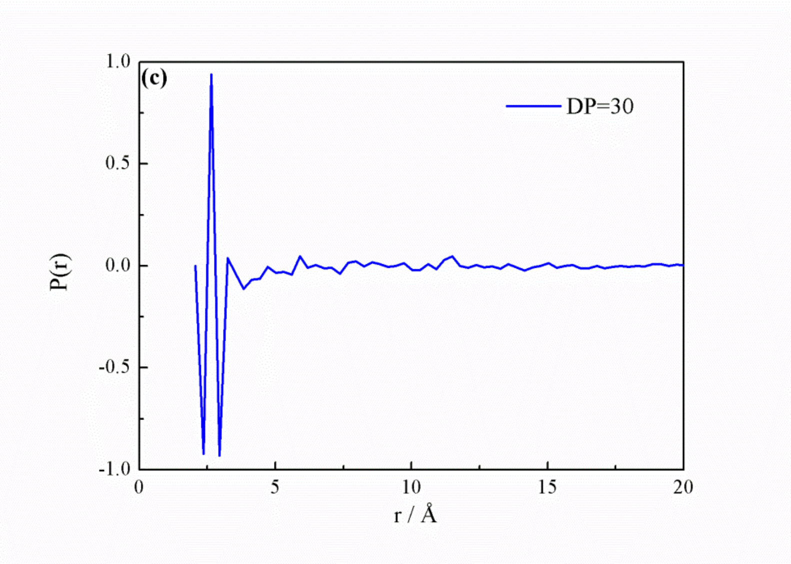

Figure 5 Orientation correlation functions of benzene rings in different chains for PPE/PS

3.2 Radii of gyration for two blends

We estimate the sizes of the molecules by the radii of gyration (R_g), and the average R_g of PPE, PMMA and PS with different combinations are listed in Table 2. Simulations of the three pure polymers were also carried out for comparison. All values of R_g are followed by their standard deviations. Here we found that when PPE is blended with PS, the R_g of both PPE and PS change little comparing to their pure forms with increasing of chain length. However, in the case of PPE/PMMA, much larger R_g of PPE were obtained when DP=20 and 30, but little change for PMMA. In order to explain this phenomenon, we analyzed the distributions of R_g in both PPE/PMMA and PPE/PS in Figure 6 and Figure 7, respectively.

Table 2 Average radius of gyrations of PPE, PMMA and PS in various systems

DP	R_g of PPE (Å)	R_g of PMMA (Å)	R_g of PS (Å)	PPE/PMMA		PPE/PS	
				R_g of PPE (Å)	R_g of PMMA (Å)	R_g of PPE (Å)	R_g of PS (Å)
5	6.3 (0.04)	4.4 (0.08)		6.8 (0.04)	4.4 (0.08)		
10	10.7 (1.26)	6.4 (0.55)	7.0 (0.27)	10.6 (1.24)	6.4 (0.54)	10.4 (0.45)	6.5 (0.28)
20	12.0 (1.66)	8.0 (1.75)	9.9 (1.36)	19.3 (3.23)	9.4 (1.76)	11.7 (2.17)	10.0 (1.34)
30	15.4 (1.82)	10.4 (1.88)	12.1 (1.70)	25.8 (4.07)	11.7 (1.92)	16.4 (3.18)	12.3 (1.74)

For the miscible system PPE/PS, wider distributions of R_g are observed for both PPE and PS when DP increases, and only one peak for each distribution can be figured out. Since PPE and PS are miscible over the whole molecular weight range, [2] there is little difference between the average R_g of PPE and PS in their pure forms and mixture.

On the other hand, for PPE in the immiscible system PPE/PMMA, the distributions of R_g for PPE become much wider with increasing chain lengths, specifically, when DP = 30, there are two peaks. For PMMA, the distributions of R_g become a little wider with the increasing of chain length, but not as much as PPE and only one peak could be found in the distribution. A snapshot of some PPE chains selected arbitrarily is shown in Figure 8 which are colored differently for easy distinction. We find the yellow and the orange chains are more stretched and the other four (pink, green, black and magenta) are more compact. PPE has a large range of conformations and neighborhoods in the immiscible system. The phenomenon mentioned above indicates that PPE and PMMA miscibility becomes weaker with increasing molecular weight. This behavior enlarges the R_g distribution of PPE but not PMMA, and the tendency of phase separation is more obvious. For DP=30, two peaks in the R_g distribution of PPE are observed, suggesting that part of PPE chains in the mixture are more stretched than those in its pure melt and there is a tendency for aggregation of PMMA chains. We can infer that the phase separation begins and PPE should be the continuous phase with a more diverse range of local neighborhoods (pure and interfacial) and PMMA is the dispersed phase at a composition of 50:50 (mol). To verify this, some snapshots are presented in Figure 9 and supplementary data. We can see some holes in the PPE phase (blue), and some clusters of red balls (PMMA), which means that there is a tendency of aggregation for PMMA and PMMA clusters are dispersed in the continuous phase PPE.

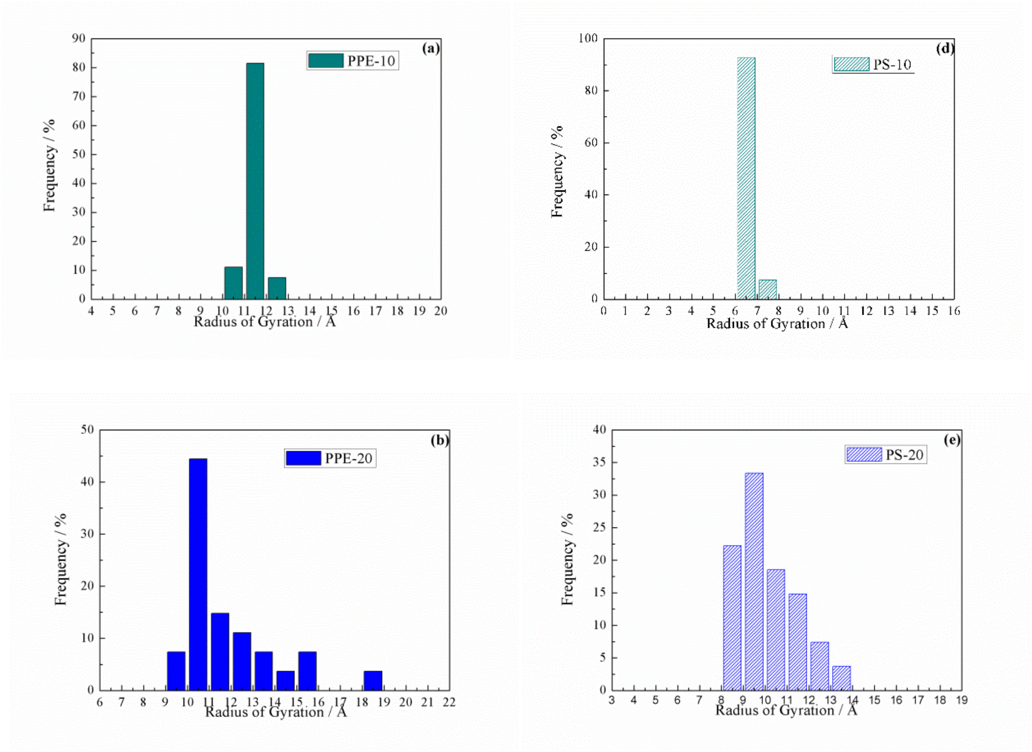

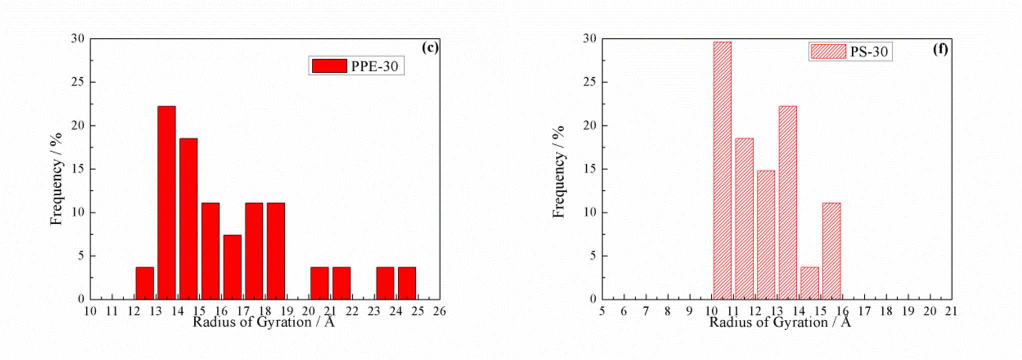

Figure 6 Distributions of R_gs in PPE/PS with different polymerization degrees

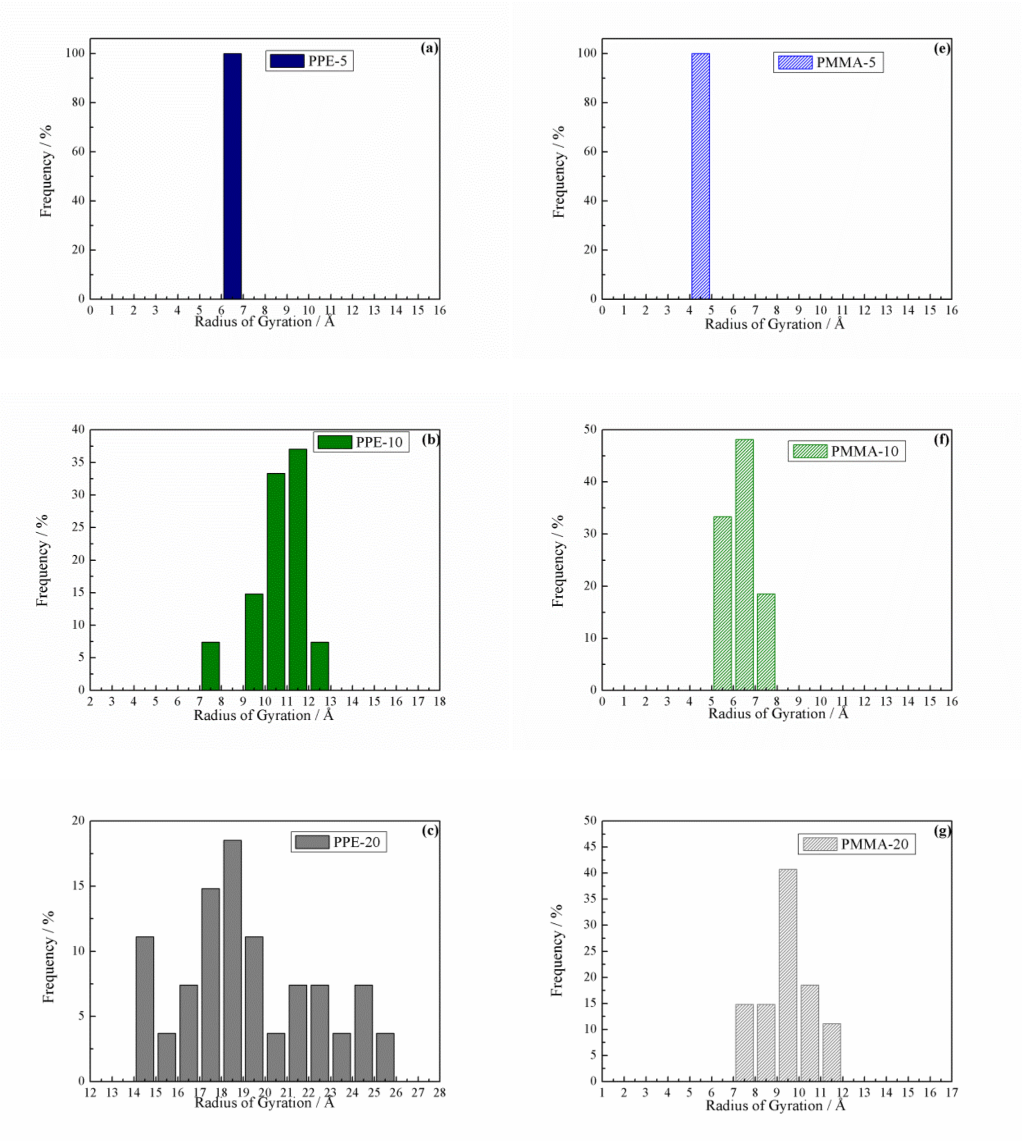

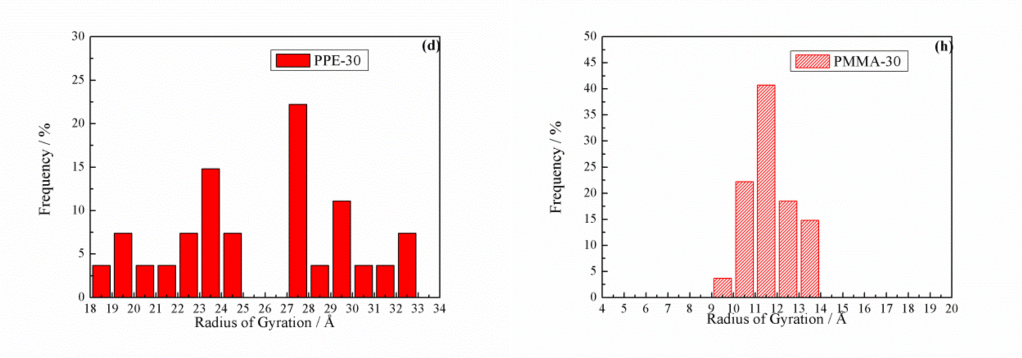

Figure 7 Distributions of R_g in PPE/PMMA with different polymerization degrees

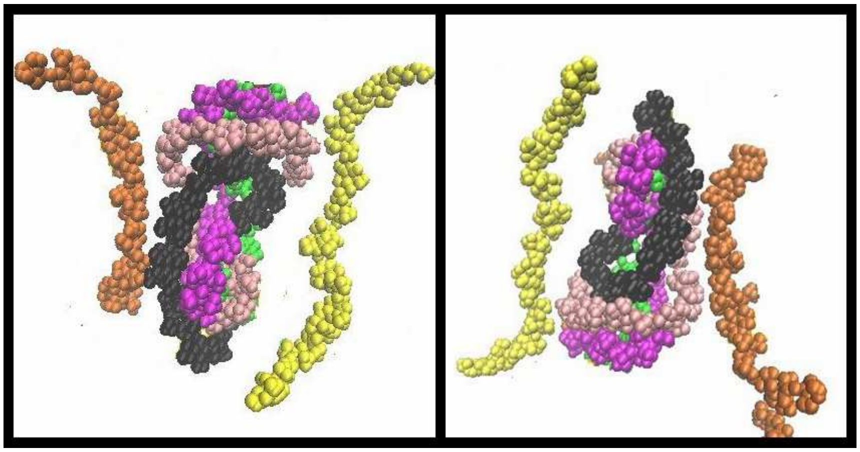

Figure 8 Snapshots of PPE chains in PPE/PMMA after 100ns equilibration (each color represents a single chain)

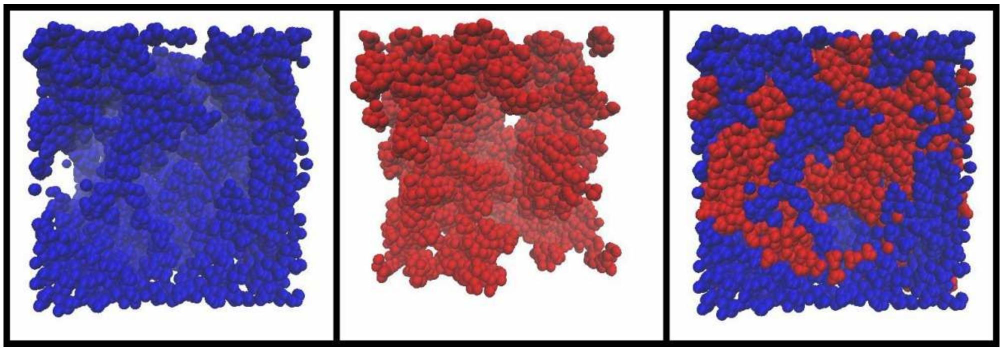

Figure 9 Snapshots of PPE/PMMA after 100ns equilibration (PPE=blue balls and PMMA=red balls)

3.3 Mean squared displacements

Mean squared displacement (MSD) analysis is a common technique to characterize motion, it can help determine whether a particle is freely diffusing or bound and limited in its movement. [44, 45] The MSD is also important to understand the mobility of monomers along the chain individually. We calculated MSD of the center-of-mass using to study the dynamics of polymer chains and monomers in chains.

The mobility of the three polymers in the two blends is largely dominated by the chemical structures and their miscibility. The flexibility of backbones has a significant impact on the mobility of polymer chains. As described in Part 3.1, PPE is the most rigid polymer, and PMMA is the most flexible one. On the other hand, the miscibility of PPE with PMMA is much weaker than PPE with PS, there are two phases in PPE/PMMA, two polymers could move in each phase which possesses relatively similar environment to their pure forms. For a miscible system, the benzene rings in PPE and PS chains can pack with each other, chains of PPE and PS tend to twine with each other so their movements are restrained for they cannot cut through each other.

Figures 10 and 11 show the influence of the position along the chain on the dynamics of monomers in two mixtures, and we found that the behavior of PPE is complex.

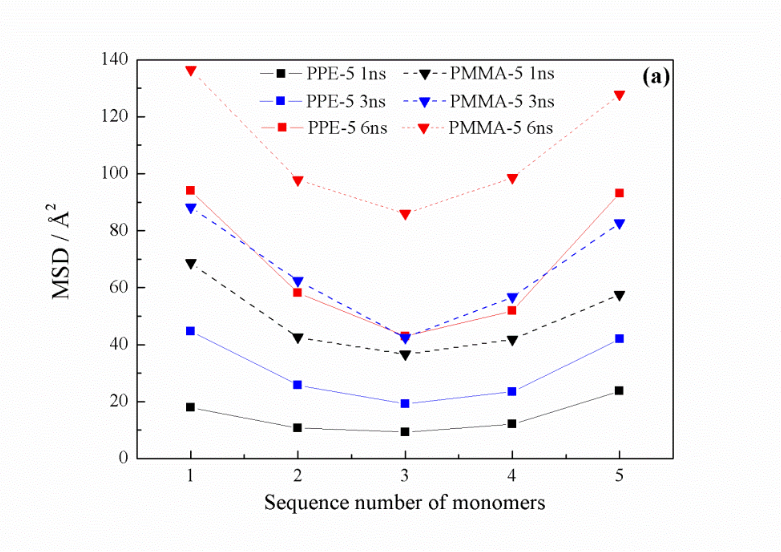
(a)
PPE-5 1ns
PMMA-5 1ns
PPE-5 3ns
PMMA-5 3ns
PPE-5 6ns
PMMA-5 6ns
MSD / Å²
0
20
40
60
80
100
120
140
1
2
3
4
5
Sequence number of monomers

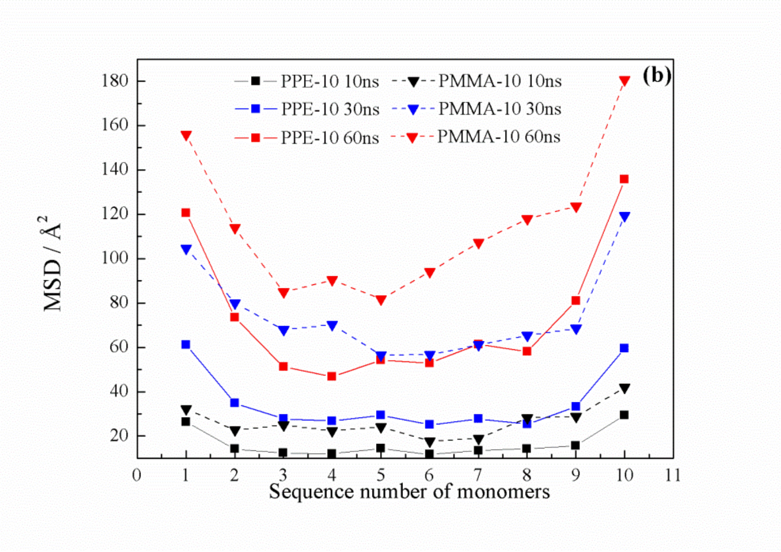
(b)
PPE-10 10ns
PMMA-10 10ns
PPE-10 30ns
PMMA-10 30ns
PPE-10 60ns
PMMA-10 60ns
MSD / Å²
20
40
60
80
100
120
140
160
180
0
1
2
3
4
5
6
7
8
9
10
11
Sequence number of monomers

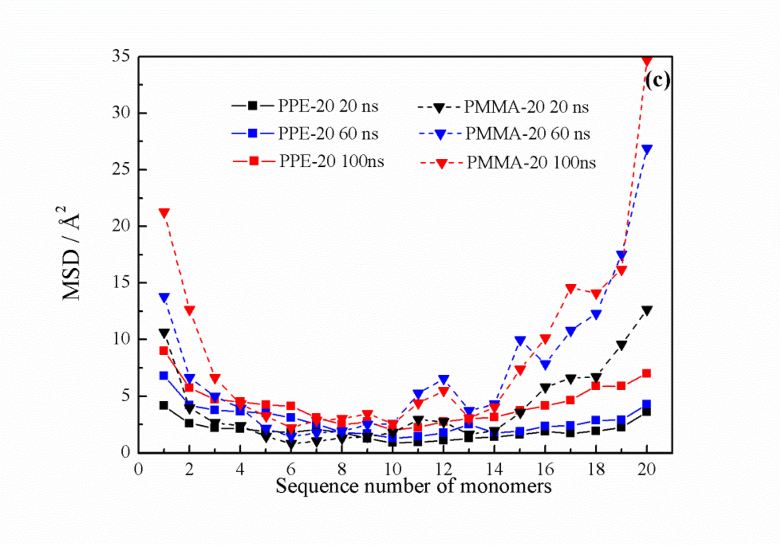
(c)
PPE-20 20 ns
PMMA-20 20 ns
PPE-20 60 ns
PMMA-20 60 ns
PPE-20 100ns
PMMA-20 100ns
MSD / Å²
0
5
10
15
20
25
30
35
0
2
4
6
8
10
12
14
16
18
20
Sequence number of monomers

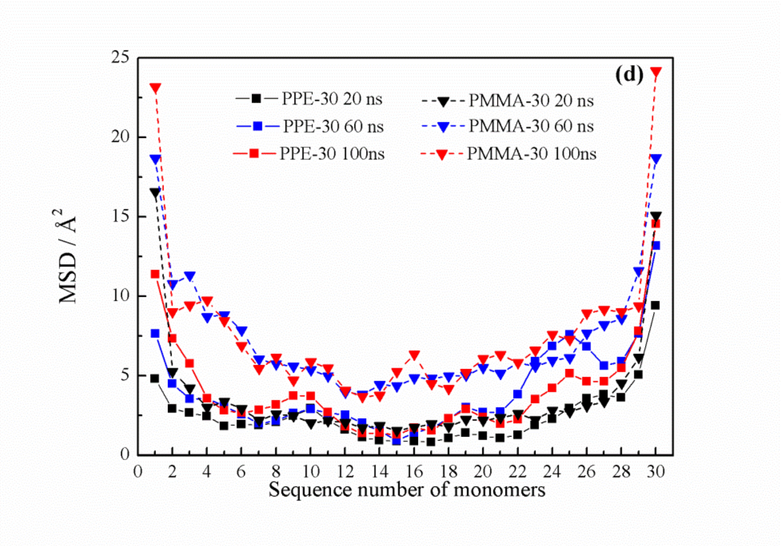

Figure 10 Mean squared displacements of all monomers along the polymer chains with different DP in PPE/PMMA

In the case of PPE/PMMA (Figure 10) for PMMA, there is a clear distinction between the monomers at the chain ends and in the center. Monomers at the end of a chain move much faster. Also monomers in PMMA chains move faster than PPE. However, for PPE the mobility of end monomers first decreases with the increasing of chain length (DP⩽20), and then increases when DP=30.

In the case of PPE/PS the end monomers also move faster than the central monomers for PS chains. There is only a minor difference between MSDs of the monomers in PPE and PS when DP=10. Monomers of PS behave similarly to PMMA. Similar to PPE/PMMA, the MSDs of monomers in PPE chains are quite small during 100 ns for DP=20, and there is only little difference between the central and end monomers. For DP=30, the end monomers become significantly faster than the central ones.

These phenomena can be explained as follows. The mobility of end monomers is influenced by two factors, the mobility of the whole chain and the distance to the central monomers. On one hand, the mobility of whole molecule decreases with the increasing of molecular weight. On the other hand, since the backbone of PPE is quite rigid and only C-O bond can rotate freely, the flexibility of chains will increase with chain lengths. When the chains are short, the motion of end monomers is slowed down by the less mobile central monomers, the central monomers will have less effect on the end monomers with the increasing of chain length. When DP⩽20, the mobility of whole chain is the leading factor, and when DP⩾20, distance between end and central monomers plays the major part.

And it can be concluded that the monomers of PPE chains in PPE/PMMA move faster than the ones in PPE/PS and monomers in PMMA move faster than those in PS when blending with PPE.

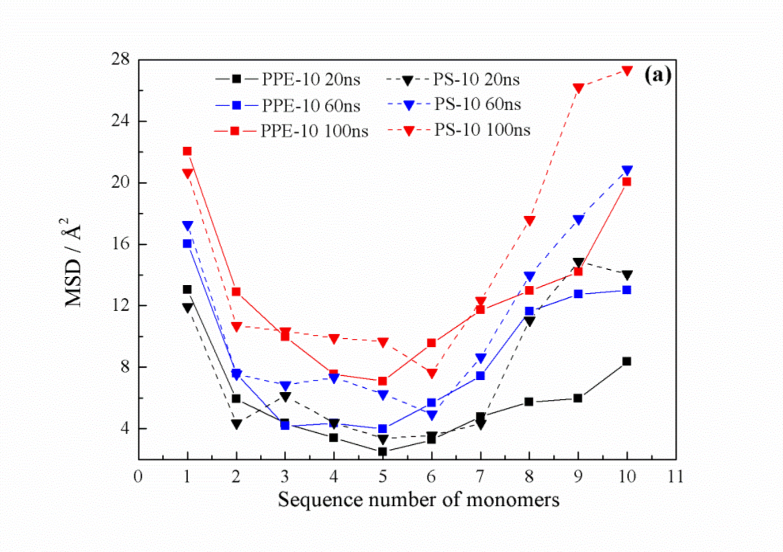

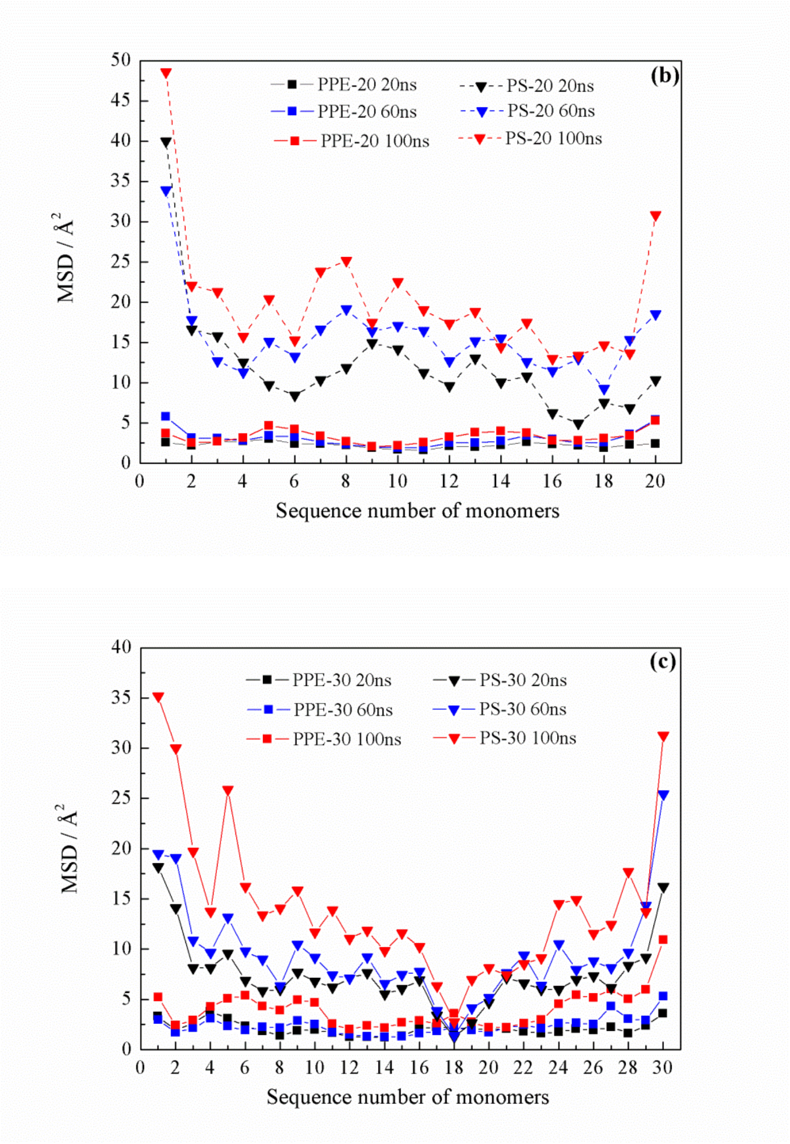

Figure 11 Mean squared displacements of the all monomers along the polymer chains with different polymerization degrees in PPE/PS

The MSDs of central monomers and whole molecules of three polymers in two blends are shown in supplementary data. As expected, MSDs of central monomers decrease rapidly with the increasing of chain length for both systems. The whole chains clearly move much more slowly than the monomers. Chain dynamics was slower in the case of PPE blended with PS compared to that with PMMA. It can be seen clearly that the MSDs of central monomers and whole molecules for PPE are smaller than the other two as expected. MSDs of central monomers for PPE in PPE/PS increase slightly as simulation time. Specifically, for PPE/PS when DP=10, the MSDs of molecules for two polymers are quite close to each other, which can correspond to the behavior of the monomers.

4. Conclusions

In the present paper, we used atomistic molecular dynamics simulations to study the different behaviors of two binary polymer blends, PPE/PS and PPE/PMMA. PPE/PS blends were observed to be miscible in all cases, which agreed with the experimental phenomenon, and this behavior might be attributed to the packing feature of the benzene rings in both polymer chains. In contrast, we found that PPE/PMMA blends were miscible for short chain lengths and phase separation appeared for longer chains. PMMA was dispersed in PPE which was the continuous phase. Furthermore, the average R_g and the R_g distributions of PPE changed when PPE was blended with PS and PMMA, respectively. The R_g distributions of PPE became wider with the increasing of chain length for PPE/PMMA, indicating some of PPE chains are fully stretched. The mobility of monomers and polymer chains in the blends was studied via the MSD. The positions of monomers along the chain could strongly affect their mobility, and the type of polymer which blended with PPE had an evident effect on the mobility of the whole chain.

In the light of this, we can conclude that the dynamics of PPE blends is sensitive not only to the molecular weight of two polymers but also to the type of the polymer.

And we can infer that a polymer blend is not just a simple combination of several polymers, since different polymers can affect each other when they are mixed together, some new properties might be achieved besides the properties possessed by pure polymers when we prepare a polymer alloy. Our study explained the experimental phase behavior on a microscopic level and should be able to bridge the gap between experimental investigation and theoretical analysis.

Acknowledgements. This study was supported by China Scholarship Council.

References

1. Hay, A. S.; Blanchard, H. S.; Endres, G. F.; Eustance, J. W. *J. Am. Chem. Soc.*, **1959**, *81*, 6335.
2. Hay, A. S. *J. Polym. Sci., Part A: Polym. Chem.*, **1998**, *36*, 505.
3. Merfeld, G. D.; Yeager, G. W.; Chao, H. S.; Singh, N. *Polymer*, **2003**, *44*, 4981.
4. Tol, R. T.; Mathot, V. B. F.; Groeninckx, G. *Polymer*, **2005**, *46*, 369.
5. Eklind, H.; Schantz, S.; Maurer, F. H. J. Jannasch, P.; Wesslen, B. *Macromolecules*, **1996**, *29*, 984.
6. Cavaille, J. Y.; Etienne, S.; Perez, J.; Monnerie, L.; Johari, G. P. *Polymer*, **1986**, *27*, 549.
7. Stoelting, J.; Karasz, F. E.; Macknight, W. *J. Polym. Eng. Sci.*, **1970**, *10*, 133.
8. Brown, H. R.; Char, K.; Deline, V. R.; Green, P. F. *Macromolecules*, **1993**, *26*, 4155.
9. Singh, S.; Frisch, H. L.; Ghiradella, H. *Macromolecules*, **1990**, *23*, 375.
10. Char, K.; Brown, H. R.; Deline, V. R. *Macromolecules*, **1993**, *26*, 4164.
11. Ayyagari, C.; Bedrov, D.; Smith, G. D. *Macromolecules*, **2000**, *33*, 6194.
12. Sun, Q.; Faller, R. *Macromolecules*, **2006**, *39*, 812.
13. Fritz, D.; Harmandaris, V. A.; Kremer, K.; Van der Vegt, N. F. A. *Polym. Phys.*, **2009**, *42*, 7579.
14. Fetters, L. J.; Lohse, D. J.; Graqessley, W. W. *J. Polym. Sci., Part B: Polym. Phys.*, **1999**, *37*, 1023.
15. Chen, C.; Depa, P.; Maranas, J.K. *J. Chem. Phys.*, **2008**, *128*, 124906.

16. Vudzien, J.; Rapheael, C.; Ediger, M. D.; de Pablo, J. J. *J. Chem. Phys.*, **2002**, *116*, 8209.

17. Heine, D.; Wu, D. T.; Curro, J. F.; Grest, F. S. *J. Chem. Phys.*, **2003**, *118*, 914.

18. Faller, R. *Macromolecules*, **2004**, *37*, 1095.

19. Sun, Q.; Faller, R. *J. Chem. Phys.*, **2007***, 126*, 144907.

20. Sun, Q.; Faller, R. *J. Chem. Theory Comput.*, **2006**, *2*, 607.

21. Bharadwaj, R. K.; Berry, R. J.; Farmer, B. L. *Polymer*, **2000**, *41*, 7209.

22. Kremer, K. *J. Chem. Phys*., **1990**, *91*, 5057.

23. Maranas, J. K.; Kumar, S. K.; Debenedetti, P. G.; Graessley, W. W.; Mondello, M. Grest, G. S. *Macromolecules*, **1998**, *31*, 6998.

24. He, Y.; Lutz, T. R.; Ediger, M. D. *J. Chem. Phys*. **2003**, *119*, 9956.

25. Plimpton, S. J. Large-scale atomic/molecular massively parallel simulator. Sandia National Laboratories, **2007**.

26. Humphrey, W.; Dalke, A.; Schulten, K. *J. Mol. Graphics*, **1996**, *14*, 33.

27. Hwang, M. J.; Stockfisch, T. P.; Hagler, A. T. *J. Am. Chem. Soc.*, **1994**, *116*, 2515.

28. Maple, J. R.; Hwang, M. J,; Stockfisch, T. P.; Dinur, U.; Waldman, M.; Ewig, C. S.; Hagler, A. T. *J. Comput. Chem.*, **1994**, *15*, 162.

29. Maple, J. R.; Hwang, M. J.; Stockfisch, T. P.; Hagler, A. T. *Isr. J. Chem.*, **1994**, *34*, 195.

30. Peng, Z. W.; Ewig, C. S.; Hwang, M. J.; Waldman, M.; Hagler, A. T. *J. Phys. Chem. A.*, **1997**, *101*, 7243.

31. Sun, H. *J. comput. Chem.*, **1994**, *15*, 752.

32. Sun, H.; Mumby, S. J.; Maple, J. R.; Hagler, A. T. *J. Am. Chem. Soc.*, **1994**, *116*, 2978.

33. Sun, H. *Macromolecules*, **1995**, *28*, 701.

34. Sun, H. *Macromolecules*, **1994**, *26*, 5924.

35. Sun, H.; Mumby. S. J.; Maple, J. R.; Hagler, A. T. *J. Phys. Chem.*, **1995**, *99*, 5873.

36. Sun, H. *J. Phys. Chem. B*, **1998**, *102*, 7338.

37. PCFF is available in LAMMPS package.

38. Fox, T. G.; Flory, P. J. *J. Appl. Phys.*, **1950,** *21*, 581.

39. Fox, T. G.; Flory, P .J. *J. Polym. Sci.*, **1954**, *14*, 315.

40. Ute, K.; Miyatake, N.; Hatada, K. *Polymer*, **1995**, *36*, 1415.

41. Gui, L.; Wang, H.; Shentu, B.; Weng, Z. *J. Appl. Polym. Sci.*, **2013**, *128*, 2919.

42. Shultz, A. R.; Beach, B. M. *Macromolecules,* **1974**, *7*, 902.

43. Adedeji, A.; Jamieson, A. M.; Hudson, S. D. Macromol. Chem. Phys. **1996**, *197*, 2521-2538.

44. Bennemann, C.; Paul, W.; Binder, K. *Phys. Rev. E*, **1998**, *57*, 843.

45. Paul, W.; Smith, G. D.; Yoon, D. Y.; Farago, B.; Rathgeber, S.; Zirkel, A.; Willner, L.; Richter, D. *Phys. Rev. Lett.*, **1998**, *80*, 2346.